

Chapter

IV

**Kinetics of Phase Transformations
in Solid Materials and Alloys**

IV-1. Introduction

There are two types of phase transformations, depending on the mode of substance transfer from the initial phase (parent phase):

Firstly, the most common type in practice involves uncoordinated atomic movements. This process leads to the destruction of the lattice structure of the original phase and the reconstruction of the lattice structure of the new phase. Phase transformations of this nature involve mechanisms for transferring substances within a solid medium, specifically diffusion. When the phase change is accompanied by a change in chemical composition, atoms move over distances that are significantly larger than the interatomic distances.

The second type involves crystallographic changes without a change in chemical composition. These transformations involve movements of atoms over short distances. The displacements are coordinated (known as *shear structures*), meaning each atom retains its neighboring atoms. An example is the martensitic transformation in steels, which produces stainless steel blades that maintain their sharpness for an extended period due to their hardness.

It is essential to study the kinetics of transformations before examining the different types of solid-state transformations in alloys.

IV-2. General characteristics of solid-state transformations

The general characteristics of phase transformation kinetics can be summarized as follows:

- a. The initiation of reactions is challenging, leading to significant delays in time or temperature, depending on whether the reaction is conducted at a constant or variable temperature.
- b. The initiation of reactions is influenced by defects in the crystal lattice and, consequently, by factors that alter the number and nature of these defects (such as hardening).
- c. The subsequent evolution of reactions is often governed by the diffusion of lattice species within the matrix. Therefore, the effect of temperature on the reaction rate primarily results from its impact on the diffusion coefficients.

These characteristics are common to most solid-state transformations that involve a change in the number of phases, which are known as first-order transformations. However, it is

challenging to draw a clear distinction between first-order and second-order transformations, as the appearance or disappearance of a phase in a solid system can sometimes occur gradually, both thermodynamically and kinetically.

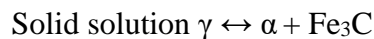
IV-3. Initiation of reactions proceeding by nucleation and growth

Among the transformations that can occur in metals or alloys in the solid state, a particularly important category is those in which a new phase forms within an initially homogeneous single-phase medium. From a purely chemical perspective, this situation can arise from various types of reactions, including:

- ❖ *Precipitation of an intermetallic compound in a supersaturated solid solution during a decrease in temperature:* An example of this type of reaction is the precipitation of the compound Al_3Mg_2 from a solid solution of Al-Mg, which is homogeneous at high temperatures, upon slow cooling.

Magnesium-rich solid solution \rightarrow Solid solution poor in magnesium + Al_3Mg_2

- ❖ *Allotropic transformation* of a pure metal through a sudden transition between stability domains: An example of this type of transformation is the cooling-induced change in iron from its gamma phase (Fe_γ , face-centered cubic or FCC) to its alpha phase (Fe_α , body-centered cubic or BCC).
- ❖ The *eutectoid transformation* of a solid solution results in the formation of two new phases rather than just one. A well-known example of this process is the formation of the eutectoid: $\alpha + \text{Fe}_3\text{C}$, within a homogeneous solid solution of 0.8% carbon in γ iron below 727°C . The transformation can be represented as:



From a morphological perspective, these different transformations begin in a similar manner. The alloy is initially heated to a high temperature where it exists as a single homogeneous phase. Upon cooling to a temperature where this phase becomes unstable, small crystalline particles of the new phase start to appear in a dispersed state. These particles grow at the expense of the matrix until, in the case of an allotropic transformation, they completely replace it.

In the case of precipitation within a supersaturated solution, the particles cease to grow once the solution reaches its new equilibrium state. This process is typically divided into two successive stages: nucleation and growth.

IV-4. Classical theory of nucleation

The theory to be developed focuses on how the stability and growth potential of a nucleus of the new phase evolve in relation to its size.

Nucleation is the phenomenon by which a new phase begins to form within the parent phase. There are two types of nucleation: homogeneous and heterogeneous. Homogeneous nucleation theoretically occurs only in a perfect crystal, where the locations of precipitate formation are indeterminate and randomly distributed within the matrix. In contrast, heterogeneous nucleation occurs at crystal defects or surfaces, which serve as preferential sites for the formation of new phases.

IV-4-1. Homogeneous nucleation

When a supersaturated solid solution (the parent phase) is allowed to evolve, concentration fluctuations occur, leading to the formation of clusters of solute at a temperature where the parent phase becomes unstable. The formation of a cluster with radius r (the new phase) alters the energy of the system. The nucleus of the new phase becomes stable only when it reaches a certain critical volume, which can be evaluated as follows:

- The free enthalpy of the initial nucleus must be less than 0 for the nucleus to be stable.
- The change in the free enthalpy of the system is the sum of three contributions:
 - 1- If ΔG_v is the change in free energy per unit volume at temperatures where the new phase is stable, then the formation of a volume V of this phase results in a decrease in free energy by $V\Delta G_v$ (noted with a negative sign in the expression for ΔG). It is important to note that ΔG_v is zero at the equilibrium temperature T_e .
 - 2- The creation of an interface with a total surface area A results in an increase in the free energy of the nucleus by $A\gamma$, where γ is the specific interfacial energy between the parent phase and the new, presumably isotropic phase.
 - 3- When the volume of the nucleus of the new phase differs from the volume initially occupied by the parent phase (which is generally the case), the free energy of the nucleus increases by an amount proportional to V , due to a stress energy per unit volume in the new phase, denoted as ΔG_c .

The total change in free energy associated with the formation of a nucleus with volume V is therefore expressed as:

$$\Delta G = -V\Delta G_v + A\gamma + V\Delta G_c = -V(\Delta G_v - \Delta G_c) + A\gamma \quad (\text{IV-1})$$

Assuming that the interface energy is independent of orientation and that the germ is spherical with a radius r , the previous equation simplifies to:

$$\Delta G(r) = -\frac{4}{3}\pi r^3 * (\Delta G_v - \Delta G_c) + \gamma * (4\pi r^2) \quad (\text{IV-2})$$

The variation in the free energy of nucleus formation thus depends on its size r (see Figure IV-1).

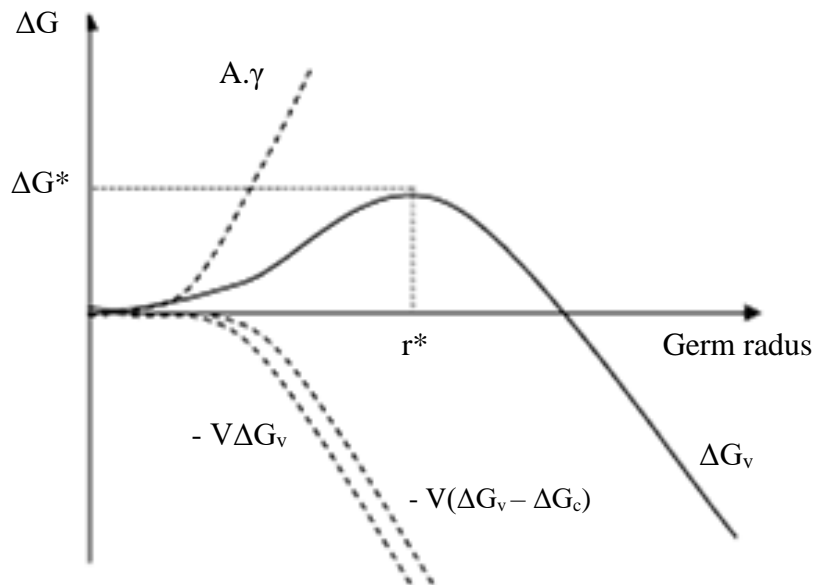


Fig. IV-1 : Evolution of the free energy of formation of a spherical nucleus as a function of its radius r .

We observe that if the size of the germs is small, the interface energy is dominant, making the germs unstable and causing them to spontaneously disintegrate within the matrix. Conversely, if the germ size is sufficiently large, the driving force becomes dominant, and the germs can evolve and become stable. Thus, there is a critical germ size threshold beyond which germination can occur and transformation can begin. By differentiating the equation for ΔG , we can determine the critical germ size r^* :

$$r^* = \frac{2\gamma}{(\Delta G_v - \Delta G_c)} \quad (\text{IV-3})$$

This yields the value of the activation free energy barrier for the formation of a critical germ:

$$\Delta G^* = \frac{16\pi\gamma^3}{3(\Delta G_v - \Delta G_c)} \quad (\text{IV-4})$$

➤ **Homogeneous nucleation rate**

Statistically, the number of germs larger than the critical size is given by:

$$N^* = N_0 \exp\left(-\frac{\Delta G^*}{KT}\right) \quad (\text{IV-5})$$

N_0 , being the number of atoms in the matrix per unit volume.

The greater the number of atoms with sufficient energy to overcome the energy barrier, the higher the probability of germ formation. This means that the germination rate is proportional to $\exp\left(-\frac{\Delta G^*}{KT}\right)$ and to the diffusion rate of the atoms to the germs $\exp\left(-\frac{\Delta G_D}{KT}\right)$.

In general, the germination rate can be expressed as:

$$V_{homo} = WN_0 \exp\left(-\frac{\Delta G_D}{KT}\right) \exp\left(-\frac{\Delta G^*}{KT}\right) \quad (\text{IV-6})$$

Where W is a factor that accounts for the vibrational frequency of the atoms.

IV-4-2. Heterogeneous nucleation

Nucleation, whether in a solid or a liquid, is often heterogeneous. Favorable germination sites include structural defects such as dislocations, grain boundaries, inclusions, free surfaces, and vacancies under supersaturation. These sites are in a non-equilibrium state, resulting in atoms in the immediate vicinity being in a higher energy state, which increases the system's free energy. If the formation of a germ of the new phase leads to the elimination of a defect, the free energy of the entire system decreases by an amount equal to the defect's free energy, ΔG_d . Thus, the defect energy plays a similar role to that of the energy per unit volume, serving as a driving force. Consequently, the expression for the variation in free energy associated with the formation of a germ of volume V is:

$$\Delta G_{\text{hété}} = -V(\Delta G_v - \Delta G_c) + A\gamma - \Delta G_d \quad (\text{IV-7})$$

An example of this type of germination is **germination on grain boundaries**:

IV-5. Description of the overall behavior of phase transformations according to Avrami's theory:

Solid-state phase transformations that proceed via a nucleation mechanism generally follow the transformation law proposed by Avrami. The Avrami treatment provides an equation that allows for the calculation of the extent of phase transformation as a function of time.

The formation and growth of a new β phase within an initial α phase can be envisioned as follows:

- Initially, at time t_0 , a germ appears within the parent phase α . This germ represents the nascent β phase. The time required for the formation of these germs is referred to as the incubation period.
- In the next stage, the germs grow at the expense of the α phase, contributing to the progress of the transformation (see Fig. IV-3). At time t_f , the transformation ceases when the initial phase is entirely converted into the new phase β . The growth of the new phase may not proceed uniformly in all directions.

The growth of the new phase proceeds freely during the initial stages of the transformation. However, this behavior changes once a certain conversion rate is reached, at which point the growing phases begin to contact each other. Taking this characteristic into account and based on the principles of nucleation and growth, we derive a general equation that describes the conversion rate (volume fraction f) as a function of the transformation time:

$$f = 1 - \exp(-K t^n) \quad (\text{IV-9})$$

This is Avrami's equation, where n varies from 1 to 4 depending on the type of transformation, and K is a function of the nucleation and growth processes, which are strongly dependent on temperature. By knowing K as a function of temperature, one can calculate the time required to achieve a specified conversion rate (e.g., 1%, 50%, 90%) at a given temperature.

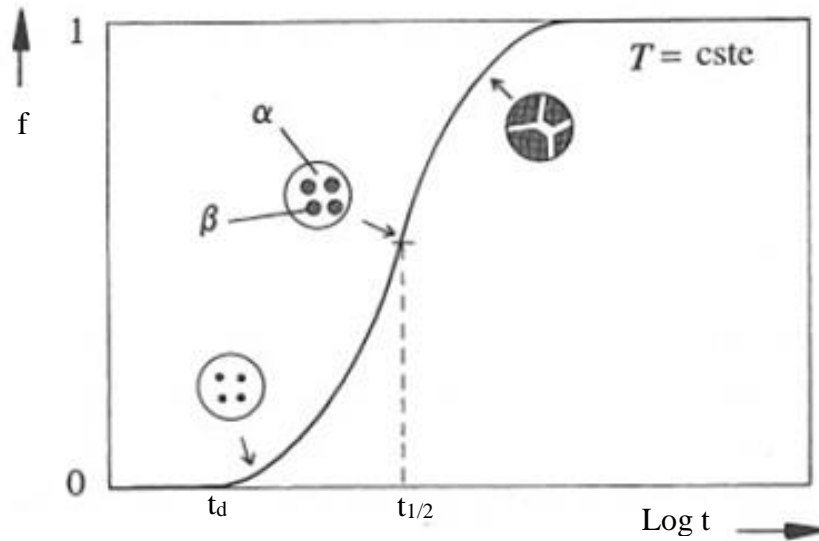


Fig. IV-3- : Isothermal variation of the volume fraction f of the transformed phase as a function of the logarithm of time t according to the Avrami equation. Here, f represents the fraction of the β phase transformed at time t , while $(1-f)$ denotes the fraction of the untransformed α phase.

IV-6. Diagrams TTT (Transformation/Time/Temperature)

From Avrami's expression, we can plot the transformation fraction (f) curves as a function of time and temperature, creating TTT (Time-Temperature-Transformation) diagrams. Typically, two conversion rates are selected, which are determined experimentally and characterize the start (e.g., 1% conversion) and end (e.g., 99% conversion) of the reaction. This is illustrated in Figure IV-4-(a). The figure shows how to determine the values of t_d and t_f at a temperature $T=T_1$ within the transformation interval. Figure IV-4-(b) establishes the relationship between the TTT diagram and the isotherm at temperature $T=T_1$. These TTT diagrams help in determining the appropriate heat treatment needed to achieve a specific structural state in a material. Although TTT diagrams can theoretically be obtained for any phase transformation, they are challenging to determine experimentally for the crystallization of metals and metal alloys due to the rapid nature of the transformation.

Reading a TTT diagram is straightforward. For example, consider selecting a temperature $T_1 < T_e$ and analyzing the progress of the transformation. After rapidly cooling (quenching) the material from $T > T_e$ down to T_1 (solid line in Figure IV-4 (a)), the material is held at a constant temperature T_1 . The transformation effectively begins at time $t=t_d$. The transformation proceeds initially at an increasing rate because the rate of transformation is proportional to the volume

transformed, as illustrated in Figure IV-4 (b). Subsequently, the transformation rate gradually decreases as the growing grains start to interact with each other.

Practically, the transformation stops when the transformed volume reaches 99% (at $t=t_f$). The dashed curve in Figure IV-4-(a) represents the end of the isothermal transformation as a function of the transformation temperature.

A typical example of a solid-solid transformation illustrated by TTT diagrams is the eutectoid transformation in steels containing 0.8% mass. C. This transformation occurs from austenite to form ferrite and iron carbides (cementite) (see Fig. IV-5).

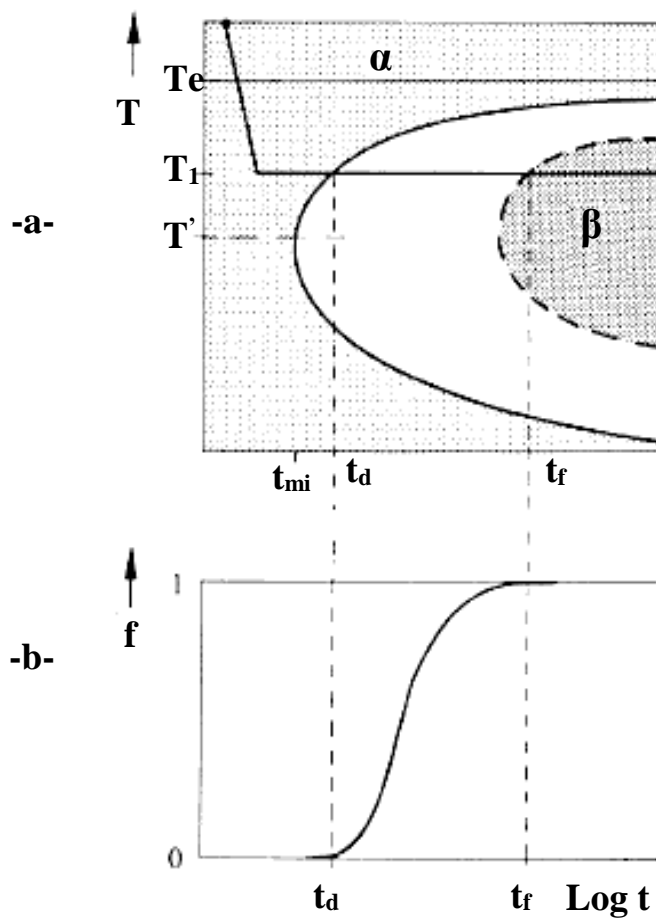


Fig. IV-4: Schematic appearance of the TTT diagram of a phase transformation: (a) Phase transformation curves as a function of time and temperature for two values of the conversion rate, characterizing the start (1% conversion, t_d) and the end (99% conversion, t_f) of the reaction. t_{min} represents the minimum time required for the transformation to commence. (b) The relationship between the TTT diagram and the transformation isotherm at temperature $T=T_1$.

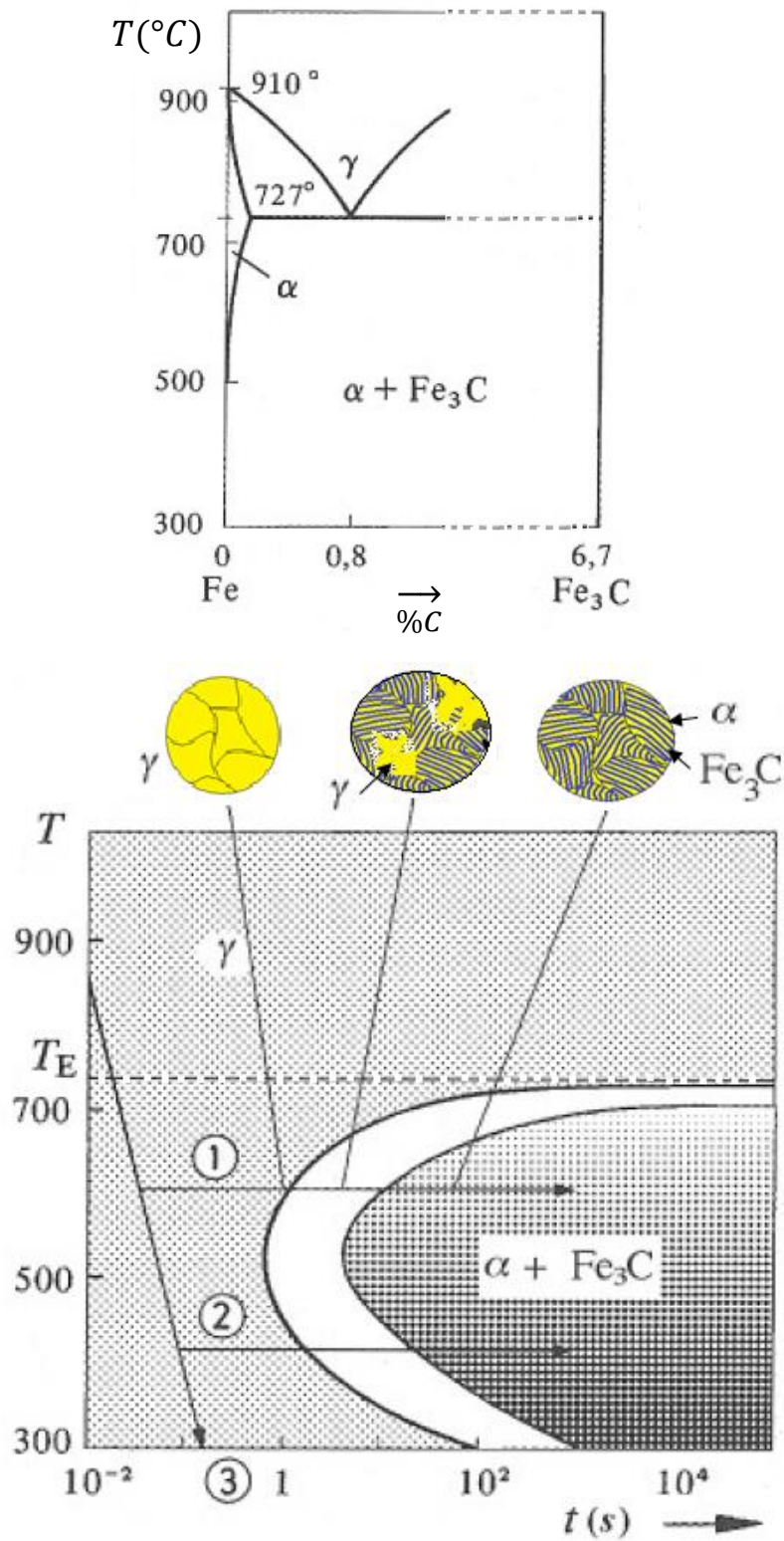


Fig. IV-5- : Part of the Fe-Fe₃C phase diagram (a) and the TTT diagram for the eutectoid transformation in this system (b).

IV-7. Spinodal decomposition theory

The previous theory attributed the delay in germination to the positive energy required for the creation of interfaces, which was considered the source of the barrier. However, an alternative analysis of the phenomenon has been known for some years, and we will briefly describe it.

IV-7-1. Definition of Spinodal decomposition

Spinodal decomposition is a phase transformation phenomenon that occurs when a continuous solid solution is cooled below a critical temperature.

Figure IV-6(a) shows the phase equilibrium diagram of the A-B binary system. Above the critical temperature and below the melting temperature, this system exists as a continuous solid solution, α .

Below T_c , an isothermal section of the diagram at temperature T' reveals three distinct zones based on the value of x (the composition of element B).

- ✓ a single-phase zone consisting of an A-rich phase α_1 for $0 < x < x_1$,
- ✓ a two-phase zone comprising both phases for $x_1 < x < x_4$,
- ✓ a single-phase zone consisting of a B-rich phase, α_2 , for $x_4 < x < 1$.

The phenomenon of isomorphic demixing in the continuous solid solution for $x_1 < x < x_4$ is illustrated in Figure IV-6(b). This figure shows the variation of the molar free enthalpy of the system as a function of composition at temperature T' .

For the two solid solutions to be in equilibrium with each other, the chemical potential of component A must be the same in both solid solutions, α_1 and α_2 . The same applies to the chemical potential of component B. The rule of the common tangent to the free molar enthalpy curve of the phase allows us to determine the compositions of the solid solution α_1 saturated with B (x_1) and the solid solution α_2 saturated with A (x_4) in equilibrium with each other.

The range of points x_1 and x_4 , obtained at different temperatures, defines a curve on the equilibrium diagram that serves as the boundary between the single-phase regions and the two-phase region. The area where the two solid solutions, α_1 and α_2 , coexist is referred to as the *miscibility gap*.

In addition to its three domains, the molar free enthalpy curve of the continuous solid solution has two points of inflection, x_2 and x_3 , which become significant when examining the mechanism of transformation from a single-phase system to a two-phase system.

In the region between the two inflection points, x_2 and x_3 , where $\partial^2 G/\partial X^2 < 0$, the single-phase solid solution is unstable and undergoes spinodal decomposition. In the composition ranges x_2-x_1 and x_4-x_3 , the single-phase solid solution is metastable and will decompose into two solid solutions through a nucleation and growth mechanism, given sufficient activation energy.

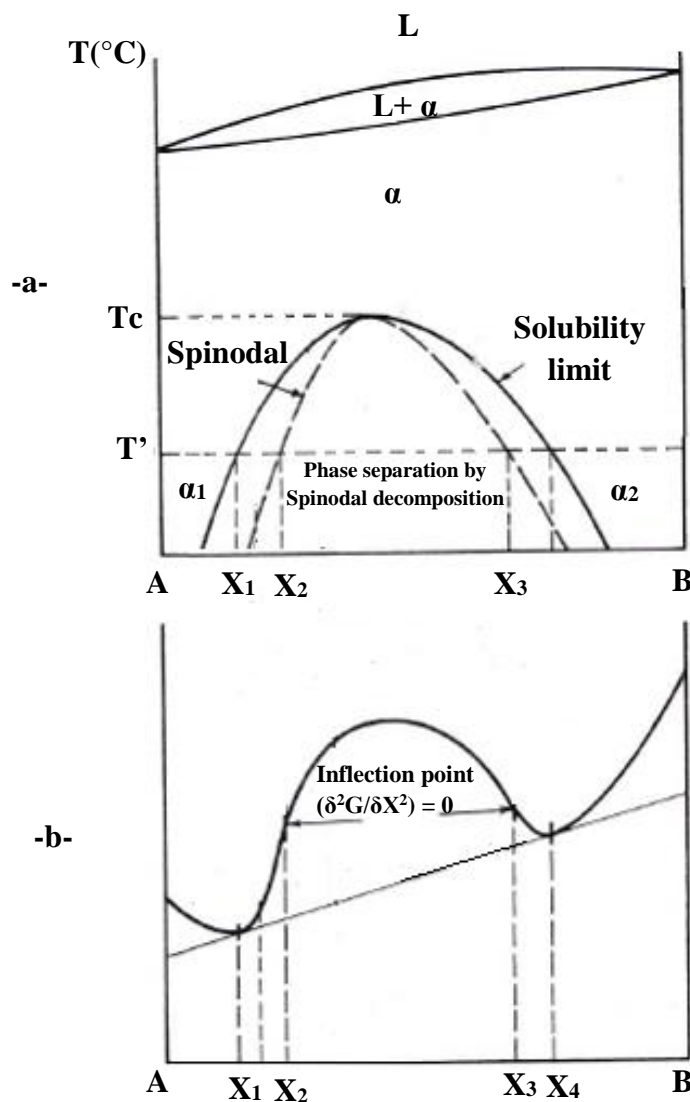


Fig.IV-6: (a) Phase diagram of a binary system showing a miscibility gap.
 (b) Variation of the free enthalpy of a solid solution at temperature T' .

IV-7-2. Mode of decomposition

To explain the mode of decomposition, we refer to the molar free enthalpy curve of the single-phase binary system at temperature T , for an average concentration X_i of element B, which is within the spinodal decomposition region (see Fig. IV-7).

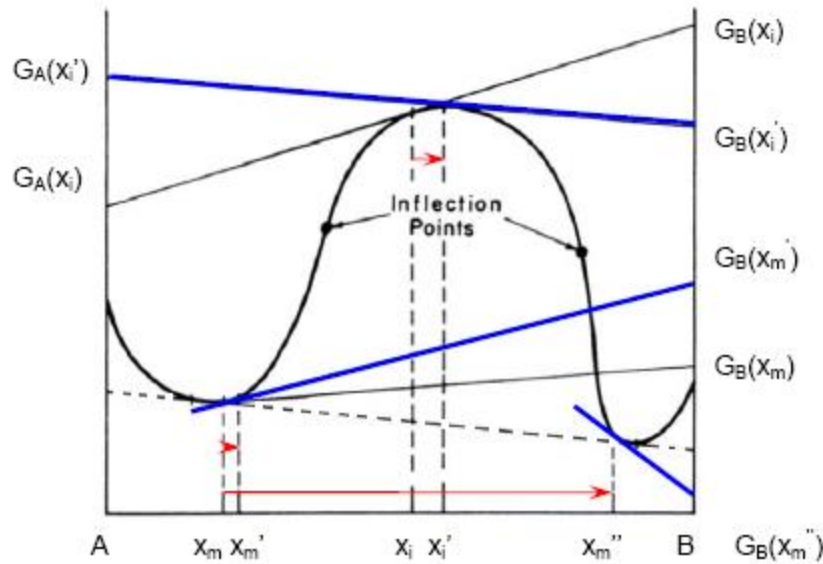


Fig. IV-7: Variation of the chemical potential as a function of composition within the miscibility range.

At a point in the solid solution, consider the emergence of a small fluctuation in composition, shifting from X_i to X_i' , which locally generates a composition gradient. This concentration gradient of element B is associated with a gradient in chemical potential, which induces a flow of matter B in the direction of decreasing chemical potential.

In Figure IV-7, the material with composition X_i has chemical potentials $G_A(X_i)$ and $G_B(X_i)$ for constituents A and B, respectively. The material with the average composition X_i' has chemical potentials $G_A(X_i')$ and $G_B(X_i')$.

In the domain of spinodal decomposition, a fluctuation in concentration from X_i to X_i' (an increase in the concentration of B) leads to a decrease in the chemical potential of component B (and an increase in the chemical potential of component A). According to Gibbs' phase rule, the B constituents adjacent to the area of composition fluctuation will diffuse into this region, which is an unusual direction of increasing concentrations, while the A constituents will move away from it. This results in regions of the material that become increasingly enriched in B and others that become increasingly depleted in B (see Fig. IV-8 (a), Stage II). This self-propagating phenomenon leads to spinodal decomposition (see Fig. IV-8 (a), Stage III).

In the metastable range at temperature T , the decomposition mechanism differs from that of spinodal decomposition. A small fluctuation in composition (transition from X_m to $X_m + dX_m$) (see Fig. IV-7 and Fig. IV-8(b), Stage I) induces a change in chemical potential from $G_B(X_m)$ to $G_B(X_m')$, with $G_B(X_m') > G_B(X_m)$. Matter flow is then directed in the usual manner, towards decreasing concentrations (see Fig. IV-7 and Fig. IV-8(b), Stage II). Consequently, this composition fluctuation eventually diminishes (see Fig. IV-7 and Fig. IV-8(b), Stage III).

In the metastable domain, for a large fluctuation in composition, such as from X_m to X_m'' , where $G_B(X_m'')$ is lower than $G_B(X_m)$, the composition fluctuation will increase. This leads to the nucleation and growth of two solid solutions with compositions X_1 and X_4 (see Fig. IV-7 and Fig. IV-8(c)).

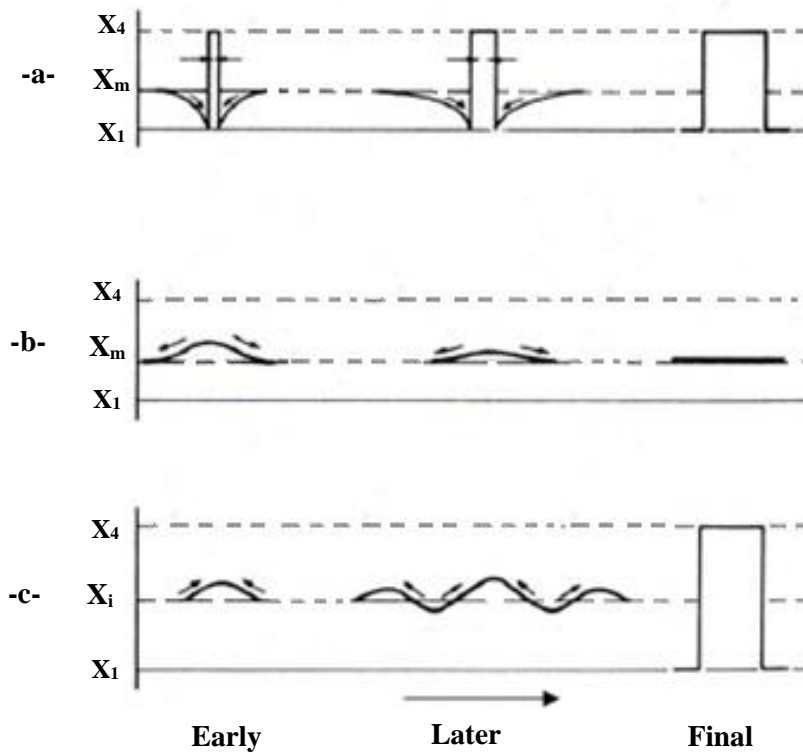


Fig. IV-8: (a) Progression of a small fluctuation within the Spinodal decomposition region,
 (b) Disappearance of a small fluctuation in the metastable phase,
 (c) Nucleation and growth of a large fluctuation in the metastable phase.

IV-8. Limitations of Previous Theories

In the discussion of the preceding theories, several factors of significant importance were neglected. This limitation notably affects the validity of the quantitative conclusions that

someone unfamiliar with the complexities of solid-state reaction kinetics might draw from the previous discussion. Therefore, it is particularly instructive to identify these simplifications and investigate how they may influence the mechanisms of transformations in each specific case.

It should be noted that the two approaches are only apparently contradictory. While the first approach emphasizes the critical role of interfacial energy, the second approach simplifies by neglecting it. However, it is possible to incorporate this energy into Spinodal theory by translating the Spinodal curve downward from its simplified form. The difference between these two curves, which can vary with temperature, represents the elastic deformation energy resulting from the parameter differences between enriched and depleted regions.

It should be noted that while classical theory introduces the concept of interfacial energy from the outset, it neglects the fact that this energy can vary significantly for the same pair of associated phases due to several factors, including:

- The morphology of the dispersed phase within the original matrix,
- The orientation relationship between the two adjacent crystal lattices,
- Constraints resulting from volume changes during processing.

Practice exercises

Exercise 1:

Consider the nucleation of a new phase β in the form of a sphere with radius r within an infinite matrix of another phase α . If nucleation occurs at grain boundaries, as shown in Figure 1,

- What is the type of Nucleation in this case?
- Provide the equation for calculating the free enthalpy of nucleation in this case, assuming that the interfacial energy (γ) of the α phase is isotropic and equal to that of the β phase.
- Calculate the critical radius value r^* .
- Calculate the wettability angle of the β phase particle on the grain boundary (θ) if $\gamma_{\alpha/\beta} = 500$ and $\gamma_{\alpha/\alpha} = 600$ mJ/m²
- Evaluate the $f(\theta)$ factor for this germ.

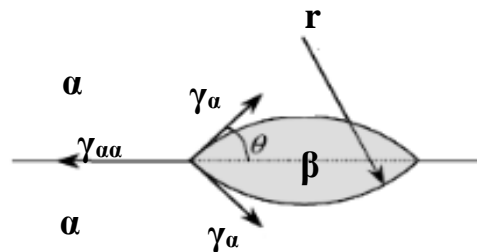


Fig. IV-9-

Exercise 2:

The isothermal transformation diagram in Fig. 2 pertains to a eutectoid steel, with phases labeled as A (austenite), B (bainite), P (pearlite), and M (martensite).

- Determine the final microstructure of a small sample subjected to the following time-temperature treatments. In each case, the initial temperature of the sample was 845°C and was held long enough for the sample to achieve a complete and homogeneous austenitic structure.
 - (a) Rapid cooling to 350°C, holding at this temperature for 104 seconds, then rapid cooling to room temperature.
 - (b) Rapid cooling to 250°C, holding at this temperature for 100 seconds, then rapid cooling to room temperature.

- (c) Rapid cooling to 650°C, holding at this temperature for 20 seconds, then rapid cooling to 400°C, holding at this temperature for 103 seconds, followed by rapid cooling to room temperature.

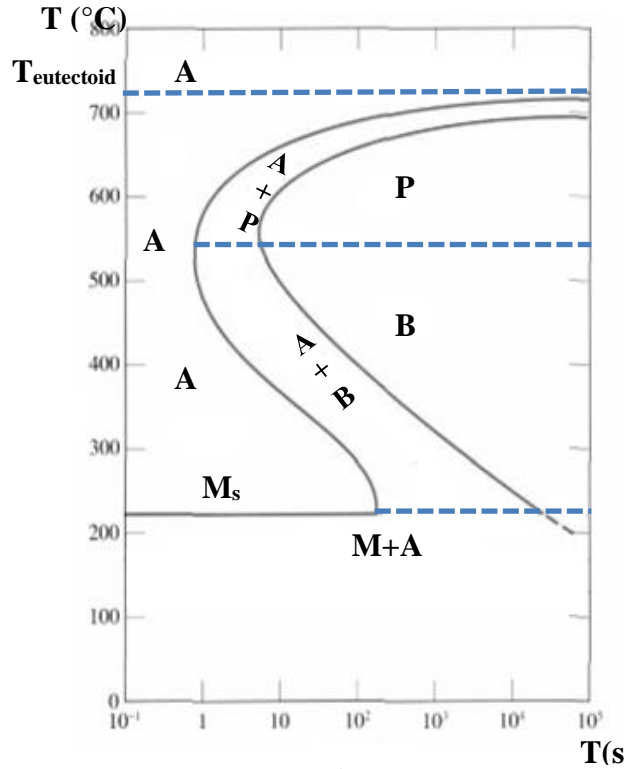


Fig. IV-10-

Exercise 3:

Solid-state phase transformation kinetics that proceed by a nucleation mechanism generally follow a transformation law proposed by Avrami. The Avrami treatment provides an equation that allows the calculation of the degree of phase transformation as a function of time.

1. If f_1 and f_2 are the fractions recrystallized at a given temperature at times t_1 and t_2 , respectively, derive a relation for n in the Avrami equation.
2. For copper, the fraction recrystallized at 135°C is given in the following table:

| Recrystallized fraction | t (s) |
|-------------------------|---------|
| 0.10 | 300 |
| 0.50 | 540 |

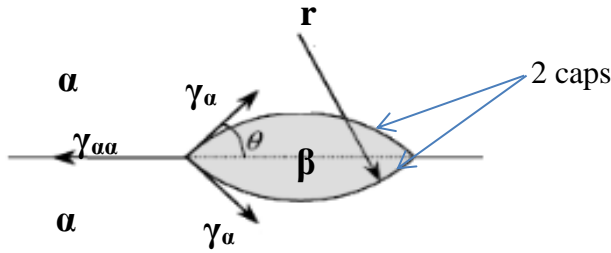
- Determine n and K in the Avrami equation

Answers

Answers for Exercise 1

- heterogeneous nucleation
- $\Delta G_{hete} = -V(\Delta G_v - \Delta G_s) + A\gamma - \Delta G_d$

In this exercise there are two spherical caps:



$$\Delta G_{hete} = -2V(\Delta G_v - \Delta G_s) + 2A\gamma_{\alpha\beta} - A_{\alpha\alpha}\gamma_{\alpha\alpha}$$

$$\gamma_{\alpha\alpha} = 2\cos\theta\gamma_{\alpha\beta}$$

$$\Delta G_{hete} = (-V(\Delta G_v - \Delta G_s) + 2A\gamma_{\alpha\beta})\left(\frac{2-3\cos\theta+\cos^3\theta}{2}\right)$$

$$\Delta G_{hete} = \Delta G_{homg} \left(\frac{2-3\cos\theta+\cos^3\theta}{2}\right)$$

$$f(\theta) = \left(\frac{2-3\cos\theta+\cos^3\theta}{2}\right)$$

$$r^* = \frac{2\gamma_{\alpha\beta}}{(\Delta G_v - \Delta G_s)}$$

$$\frac{\Delta G_{hete}^*}{\Delta G_{homg}^*} = f(\theta)$$

The grain boundary ability of decreased ΔG_{hete}^* depends on the angle $\theta \leftrightarrow \frac{\gamma_{\alpha\alpha}}{2\gamma_{\alpha\beta}}$

Si $\gamma_{\alpha\beta}=500 \text{ mJ/m}^2$ et $\gamma_{\alpha\alpha} = 600 \text{ mJ/m}^2$

The wettability angle θ is : $\theta = 33,56^\circ$

$$f(\theta) = 0.208$$

Answers for Exercise 2

The temperature change curves versus time for the three treatments are shown in Fig. IV-11-

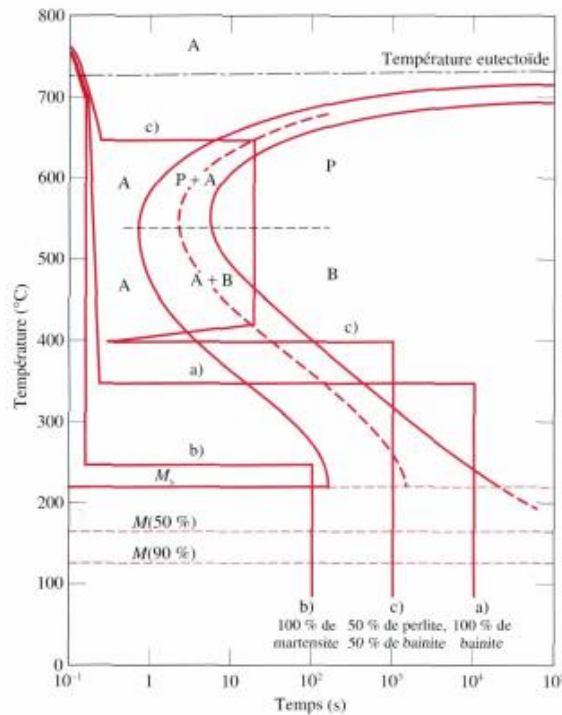


Fig. IV-11-

- a) At 350°C, the transformation of austenite into bainite is isothermal. It begins after about ten seconds and ends approximately 500 seconds later. Therefore, after the 10⁴ seconds specified in the problem, the sample contains only bainite. This means that no further transformation is possible, even if the subsequent rapid cooling curve crosses into the region of the diagram corresponding to martensite.
- b) At 250°C, the transformation to bainite begins after approximately 150 seconds. This means that after 100 seconds, the sample still contains only austenite. Once cooling lowers the sample temperature to about 215°C or below, the instantaneous transformation of austenite to martensite begins and progresses. As a result, when the sample reaches room temperature, the final microstructure consists solely of martensite.
- c) In the case of the isothermal curve at 650°C, pearlite formation begins after approximately 7 seconds. After 20 seconds, about 50% of the austenite initially present in the sample has transformed into pearlite. The vertical line represents the rapid cooling to 400°C, during which the amount of austenite transforming into pearlite or bainite is very small or even zero,

despite the cooling curve passing through the regions of the diagram corresponding to pearlite and bainite. At 400°C, the elapsed time measurement is reset to zero. After 10 seconds, the austenite that was still present in the sample (about 50%) has completely transformed into bainite. Since no austenite remains in the sample, any further transformation is impossible during the rapid cooling to room temperature. The final microstructure thus consists of pearlite and bainite in equal proportions, with 50% of each.

Answers for Exercise 3

1. $f = 1 - e^{-(Kt)^n}$

$$n \ln\left(\frac{t_2}{t_1}\right) = \ln\left(\frac{\ln(1-f_2)}{\ln(1-f_1)}\right)$$

$$n = \frac{n\left(\frac{\ln(1-f_2)}{\ln(1-f_1)}\right)}{\ln\left(\frac{t_2}{t_1}\right)}$$

2. Determination of n and K:

$$\ln\ln\left(\frac{1}{1-f}\right) = n \ln t + \ln K$$

Solving gives n=3.22

K= 1.11x10⁻⁹.s^{-3.22}